GATING CURRENT HARMONICS

II. Model Simulations of Axonal Gating Currents

JURGEN F. FOHLMEISTER*‡ AND WILLIAM J. ADELMAN, JR‡
*Laboratory of Neurophysiology, University of Minnesota, Minneapolis, Minnesota 55455; and
‡Laboratory of Biophysics, National Institute of Neurological and Communicative Disorders and Stroke, National Institutes of Health at the Marine Biological Laboratory, Woods Hole, Massachusetts 02543

ABSTRACT A kinetic model of sodium activation gating is presented. The kinetics are based on harmonic analysis of gating current data obtained during large-amplitude sinusoidal voltage clamp in dynamic steady state. The technique classifies gating kinetic schemes into groups based on patterns of the harmonic content in the periodic gating current records. The kinetics that simulate the experimental data contain two independently constrained processes. The model predicts (*a*) sizable gating currents in response to hyperpolarizing voltage steps from rest; (*b*) a substantial increase in the initial peak of the gating current following voltage steps from prehyperpolarized potentials; (*c*) a small delay in the onset of sodium ion current following voltage steps from prehyperpolarized potentials; and (*d*) flickering during the open state in single channel current records. Although fundamentally different in kinetic structure from the Hodgkin-Huxley model, the present model reproduces the phenomenological development of Na conductance during the initiation and development of action potentials. The implications for possible gating mechanisms are discussed. A model gate is presented.

INTRODUCTION

The companion paper (Fohlmeister and Adelman, 1985) gives the results of a specific harmonic analysis of gating currents in squid giant axons. The currents were elicited by sinusoidal voltage clamp of one amplitude (±35 mV) with the mean membrane potential, E_{mean}, of the sinusoid and the sinusoidal frequency as independent variables. For given values of the independent variables the sinusoid was maintained until the gating current response was periodic with the period of the voltage sinusoid. The periodic state is approached asymptotically and is termed "dynamic steady state." In contrast to frequency-domain analysis of gating currents generated by noise stimuli (Takashima, 1978; Taylor and Bezanilla, 1979; Fernandez, Bezanilla, and Taylor, 1982), current records generated in dynamic steady states give the sources of various nonlinearities (e.g., saturation plateaus, bimodal distribution within one period, current surges) by direct inspection. The model kinetics that are constructed herein are based on this direct information. The detailed harmonic content in the data records is then used for parameter adjustment.

Current records in dynamic steady state show the striking development of a strong second harmonic component as a function of E_{mean}; as E_{mean} is increased to values above −40 mV a second outwardly directed peak develops in the current records during the falling phase of the command sinusoid. For values of E_{mean} between −40 and −10 mV the amplitude of the second harmonic component of the periodic records varies very nearly in proportion to m_∞^3 of the Hodgkin-Huxley (1952) model as a function of E. Nevertheless, the Hodgkin-Huxley model, as well as other basic kinetic models that describe the time development of sodium conductance, show no trace of a corresponding second harmonic component (see Fohlmeister and Adelman, 1985, Appendix). The patterns of harmonic content generated by those models are sufficiently similar that they may be considered dynamically equivalent, although differences in detail do appear. The challenge, therefore, is to find a set of model gating kinetics that is dynamically equivalent to those that generate the experimental harmonic components.

A very simple way to do this mathematically is to assign negative weighting to the final kinetic transition that occurs in standard gating kinetic schemes following a step depolarization as, for example, the transition $x_3 \rightleftharpoons x_4$ in Eq. 1a of Fohlmeister and Adelman, 1985. The question then becomes one of the physical interpretation of the negative weighting. If one assumes that a single charged entity acts as generator of gating current then the direction of movement (component normal to the plane of the membrane) of that charge must reverse in the final kinetic

Send correspondence to Dr. Jurgen Fohlmeister, Physiology Department, 6-255 Millard Hall, 435 Delaware Street, SE, University of Minnesota, Minneapolis, MN 55455

transition. That final transition would be due to the steric changes in the channel molecule resulting from the transitions leading up to it, and would imply a charge movement against the externally applied electric field. Such a charge movement cannot be ruled out on electrostatic grounds because local charges within the molecule could contribute the dominant component of the local electric field. However, once the molecule is in that end state it is difficult to see how a reversal of the external field (i.e., repolarization) could coax the molecule out of that state because such a kinetic transition would require the gating particle (charge) to move against the components of both the externally applied and local fields.

This objection is removed by assuming two charges, each of which is associated with one of two moving molecular components. The motion of one component is in response to changes in the external electric field, and implicitly causes a change in the local field due to the steric rearrangement. The second charge responds to the altered local field with a directional component of movement that is opposed to the external field component, but in a direction compatible with the net local field. Thus, the physical objection raised above is removed by assuming a separate voltage-sensitive process that alters the local field. The movement of both charges contributes to the gating current; however, the direction of motion of the second charge is equivalent to negative weighting in generating its current component.

The recent determination of the amino acid sequence of the sodium channel in electroplax (Noda et al., 1984) shows four repeating subunits, each of which may be involved with gating. The model process described above may therefore occur at four channel locations in parallel. Following a detailed analysis of model kinetics in the Results, a hypothetical gating mechanism based on the amino acid residue sequence is given in the Discussion.

RESULTS

A Basic Kinetic Model

To explain the pattern of behaviors of the harmonic data in Fohlmeister and Adelman (1985), it is necessary to introduce gating kinetics that give a centrally located peak in the amplitude of the second harmonic on the axis of mean membrane potentials (see Fohlmeister and Adelman, 1985). On the basis of the foregoing arguments we therefore propose the following set of kinetic equations as the simplest model to account for that feature and other details in the harmonic data:

$$\dot{x}_1 = -k_{12}x_1 + k_{21}x_2 \tag{1a}$$

$$\dot{x}_2 = -(k_{23} + k_{21})x_2 + k_{32}x_3 + k_{12}x_1 \tag{1b}$$

$$\dot{x}_3 = -(k_{34} + k_{32})x_3 + k_{43}x_4 + k_{23}x_2 \tag{1c}$$

$$\dot{x}_4 = -(k_{45} + k_{43})x_4 + k_{54}x_5 + k_{34}x_3 \tag{1d}$$

$$\dot{x}_5 = -k_{54}x_5 + k_{45}x_4 \tag{1e}$$

$$\dot{x}_0 = -\kappa_{06}x_0(x_1 + x_2 + x_3 + x_4) + \kappa_{60}x_6x_5 \equiv -k_{06}x_0 + k_{60}x_6 \tag{1f}$$

$$\dot{x}_6 = -\kappa_{60}x_6x_5 + \kappa_{06}x_0(x_1 + x_2 + x_3 + x_4) \equiv -k_{60}x_6 + k_{06}x_0, \tag{1g}$$

where the rate constants k_{06} and k_{60} are parametrized as

$$k_{06} \equiv \kappa_{06}(x_1 + x_2 + x_3 + x_4) \tag{2a}$$

and

$$k_{60} \equiv \kappa_{60}x_5. \tag{2b}$$

The Eqs. 1 are constrained by two independent conditions

$$x_1 + x_2 + x_3 + x_4 + x_5 = 1 \tag{3a}$$

and

$$x_0 + x_6 = 1, \tag{3b}$$

which reflects the physical distinctness (i.e., the independent degrees of freedom) of the two moving components that are functionally coupled.

The set of nine equations (Eqs. 1 and 3) overdetermines the seven functions x_0 through x_6. These functions represent population probabilities of seven molecular substates. In computing the population probabilities Eq. 3a may replace any one of the Eqs. 1a through 1e and Eq. 3b may replace either Eq. 1f or 1g.

The model describes the behavior of a pair of coupled transition processes. The primary process

$$x_1 \rightleftharpoons x_2 \rightleftharpoons x_3 \rightleftharpoons x_4 \rightleftharpoons x_5 \tag{4a}$$

is strictly voltage dependent with depolarizations causing a shift to the right in the population of states x_1 through x_5. The secondary process

$$x_6 \underset{k_{06}}{\overset{k_{60}}{\rightleftharpoons}} x_0 \tag{4b}$$

responds to the population shift within the primary process by changing the population of x_0 at a rate equal to the difference of two terms: The term tending to increase the population of x_0 is proportional to the population of state x_5, and the term tending to decrease the population of x_0 is proportional to the sum $x_1 + x_2 + x_3 + x_4$ (see Eqs. 2). Thus, the main force that affects transitions $x_6 \rightleftharpoons x_0$ in a given molecule is a transition in the molecular substates of the primary process between x_4 and x_5. Population shifts among substates x_1, x_2, x_3, and x_4 will not directly affect transitions within the secondary process. Thus, the secondary transitions $x_6 \rightleftharpoons x_0$ are assumed to be mainly due to steric changes in the molecule as a result of a specific transition in the primary process. However, because transitions $x_6 \rightleftharpoons x_0$ must contribute to the gating current, they must be accompanied by a charge movement. Since

charges are involved in the second process, the factors κ_{06} and κ_{60}, and therefore the rate constants k_{06} and k_{60}, will likely have a direct voltage dependence of their own. However, the voltage dependence of the rate constants k_{06} and k_{60} may be considerably weaker than that of the rate constants of the primary process because voltage (across the membrane) is not considered to be the main force that is driving the transitions $x_6 \rightleftharpoons x_0$.

The model thus assumes ten overall molecular conformations: two (x_0 or x_6) for each of the states of the primary process. However, some of the ten conformations will occur considerably more rarely than others; various physical interpretations of the kinetic equations are given in the Discussion.

Harmonic Analysis of the Model

The fit to the harmonic data that is given in Fig. 1 was achieved by assigning the following values to the rate constants

$$k_{12} = (97.6)\mathrm{a}(E) \tag{5a}$$

$$k_{23} = (11.52)\mathrm{a}(E) \tag{5b}$$

$$k_{34} = (5.76)\mathrm{a}(E) \tag{5c}$$

$$k_{45} = (3.2)\mathrm{a}(E) \tag{5d}$$

$$k_{21} = (0.19)\mathrm{b}(E) \tag{5e}$$

$$k_{32} = (0.51)\mathrm{b}(E) \tag{5f}$$

$$k_{43} = (1.54)\mathrm{b}(E) \tag{5g}$$

$$k_{54} = (6.08)\mathrm{b}(E), \tag{5h}$$

where

$$\mathrm{a}(E) = \frac{-0.07E}{\exp[-0.07E] - 1} \tag{6a}$$

and

$$\mathrm{b}(E) = \exp[-0.04E] \tag{6b}$$

and

$$\kappa_{60} = 200 \exp(-0.016E) \tag{7a}$$

$$\kappa_{06} = 200 \exp(0.016E). \tag{7b}$$

For the curves in Fig. 2 all rate constants are identical to the above except

$$\kappa_{60} = 50/[\exp(-0.01\,E) + 1] \tag{7c}$$

$$\kappa_{06} = 50[\exp(-0.01\,E) + 1]. \tag{7d}$$

Note that κ_{60} and κ_{06} are relatively large. Therefore, the rate constants k_{60} and k_{06} will also be relatively large under certain circumstances (their actual values will depend on the populations of state x_5 and the sum $x_1 + x_2 + x_3 + x_4$; see Discussion). The large magnitudes of κ_{06} and κ_{60} give a tight coupling of the secondary process to the primary process.

The gating current, i_g, is given by:

$$i_g = 6.0\,[x_1k_{12} + x_2k_{23} + x_3k_{34} + x_4k_{45} - x_5k_{54} - x_4k_{43} - x_3k_{32} - x_2k_{21} + 2.0\,(x_0k_{06} - x_6k_{60})\,], \tag{8}$$

where the units of the proportionality factor, 6.0, are

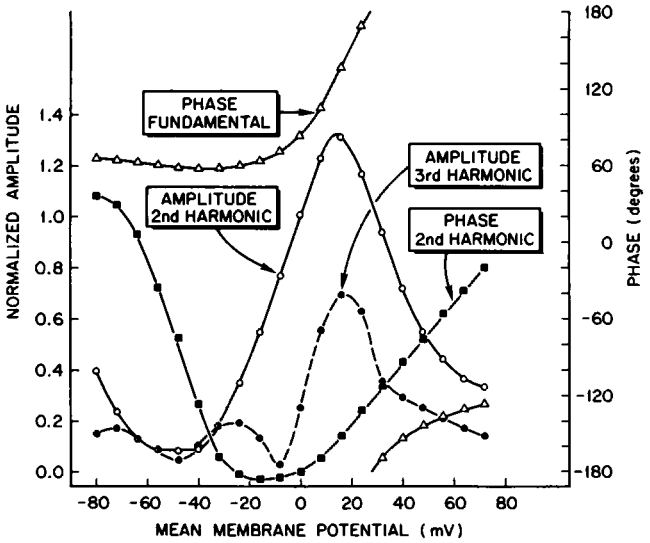

FIGURE 1 Phase of the fundamental component (△) and amplitude (○) and phase (■) of the second harmonic (solid curves) as functions of E_{mean} of the periodic gating current (Eq. 8) generated by the kinetic model (Eqs. 1, 2, 3, and 4) with rate constants as in Eqs. 5, 6, and 7 (*a* and *b*) for a steady state frequency of 500 Hz with a sinusoidal voltage amplitude of 35 mV. Dashed curve gives the third harmonic amplitude for the same conditions (•). Parameters were adjusted to match the data given in Fig. 7 of Fohlmeister and Adelman (1985).

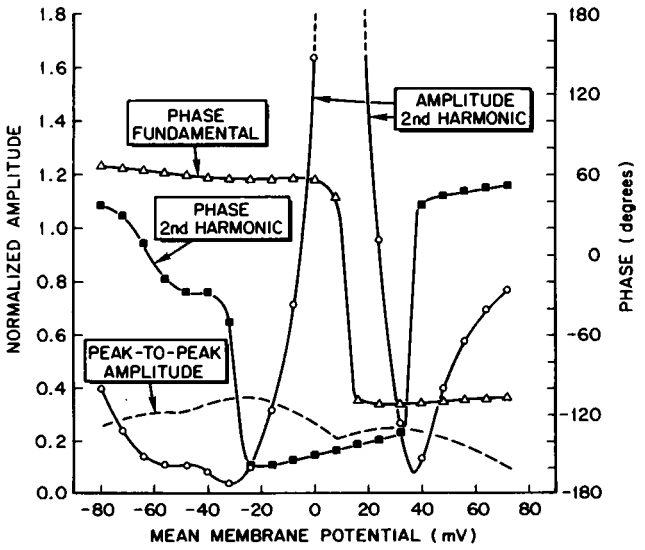

FIGURE 2. Same as Fig. 1 except for changes in the voltage dependence of the rate constants of the secondary kinetic process given by Eqs. 7c and 7d, and dashed curve gives the peak-to-peak amplitude of the simulated gating current.

nano-Coulombs/cm^2, those of the rate constants k_{ij} are in inverse milliseconds, and the x_i are dimensionless population probabilities to yield i_g in micro-Amperes/cm^2.

This kinetic model is exceedingly robust in its determination to generate the basic harmonic features of the data. Three features are considered as basic. (*a*) The amplitude of the second harmonic must peak strongly near the center of the mean membrane potential range. (*b*) The phase of the second harmonic must decline to a broad minimum in the region of the amplitude peak, and (*c*) The phase of the fundamental component must make a reasonably sharp transition from a positive value to a negative value within the region of the peak of the second harmonic amplitude.

To illustrate an important effect of parameter variation and the robustness of the model with regard to its basic harmonic features, Fig. 2 gives the results of the harmonic analysis of the kinetic model with the direct voltage dependence of the secondary process altered (see Eqs. 7c and 7d). In comparing Figs. 1 and 2 at least the following points are of importance; each of these points has been verified in numerous other simulations.

(*a*) The presence of the centrally located peak in the normalized amplitude of the second harmonic is an innate feature of the kinetic model that is virtually independent of the values of parameters.

(*b*) The phase of the second harmonic is substantially reduced in the region of the amplitude peak. Note also in Fig. 2 that this model phase behavior is somewhat unstable in regions of mean membrane potential where the phase changes most rapidly (see point *c* below).

(*c*) The phase of the fundamental component shows two types of behavior in the region between 0 and +20 mV. These divergent behaviors are due to the phase instability noted in Fohlmeister and Adelman (1985).

(*d*) In regions of phase stability the phases of the fundamental and second harmonic show an overall increase when the values of the primary rate constants are increased. Increasing the rate constants is, to a certain extent, equivalent to decreasing the command voltage frequency, and vice-versa. The reduced phase values observed in the experimental data for the higher command frequencies are due to this phenomenon.

(*e*) Endowing the rate constants of the secondary process with a voltage dependence of the sense given in Eqs. 7a and b severely blunts the sharpness of the peak in the amplitude of the second harmonic (Fig. 1). It also moderates the rolloff in that amplitude as the mean membrane potential increases towards the upper end of the data range (compare Figs. 1 and 2). Both of these properties are consistent with the experimental data. However, the experimental amplitude peak assumes a more pointed shape for higher frequencies (3 to 5 kHz, see Fohlmeister and Adelman, 1985, Figs. 9 and 10). Thus, the direct voltage dependence of the secondary rate constants appears to be weakened when the kinetic system is driven at the higher command frequencies.

(*f*) The width of the peak in the amplitude of the second harmonic tends to increase under the following two conditions: (i) increasing the voltage dependence of the rate constants of the secondary process (i.e., increasing the magnitude of the numerical coefficients in the exponents of Eqs. 7a and b), and (ii) increasing the values of the rate constants of the primary process.

(*g*) For parameters as in Fig. 1 (i.e., Eqs. 6 and 7a and b) the height of the peak of the amplitude of the second harmonic increases (or decreases) systematically when the magnitudes of the rate constants κ_{06} and κ_{60} (i.e., the factors 200 in Eqs. 7a and b) are increased (or decreased), respectively. The dependence is relatively weak, with the normalized amplitude peak decreasing from 1.33 to 1.24 when the rate constants k_{06} and k_{60} are halved, with little distortion in other regions of the curve or in other harmonic components.

Parameter Determination

Parameter values were bracketed by the following procedure: The value of the rate constant $k_{45} = 3.2$ ms^{-1} at 0 mV was chosen to give the known response time of Na-activation gating to voltage steps (see Hodgkin and Huxley, 1952). All other rate constants of the primary process were adjusted in order to adequately depress the amplitude of the second harmonic at the high and low ends of the range of mean membrane potentials (see Fohlmeister and Adelman, 1985, Appendix). This required, in particular, the relatively large ratio of k_{12}/k_{21} and the relatively large value of $k_{54} = 6.08$ ms^{-1} when compared with the analogous values of the Hodgkin-Huxley model at 0 mV (Fohlmeister and Adelman, 1985). The voltage dependences of the primary process, given by Eqs. 6, were adjusted to give a reasonable difference in Na activation between −60 and 0 mV. The parameters of the secondary process were chosen to correctly round off the peak in the second harmonic amplitude when compared with biological data. Both the amplitude and phase of the second harmonic for $E_{mean} > +10$ mV fell into place as a byproduct of this adjustment.

In all, 96 computations such as those leading to Figs. 1 and 2 were carried out on a Cyber 845 computer (Control Data Corp., Minneapolis MN) for the purposes of determining model properties and for adjusting model parameters. In general, adjustments in specific rate constants within the primary process had a dominant influence in altering the harmonic behavior (in particular the amplitude and phase of the second harmonic) in specific regions of mean membrane potential: Changes in the rate constants near the left (or right) end of the kinetic diagram in Eq. 4a had a dominant influence near the low (or high) end of membrane potentials, respectively. Given the five-state primary kinetic process, we were satisfied with the behavior of the model for mean membrane potentials greater than about −55 mV. This range includes the range of

influence of the secondary process. For membrane potential values < -55 mV the phase of the fundamental does indeed behave correctly; however, we could not obtain a simultaneous fit in amplitude and phase of the second harmonic (compare Fohlmeister and Adelman, 1985 Fig. 7 with Fig. 1 herein). Within the basic confines of the model presented herein, the necessary corrections will appear as a change in the kinetic structure near the left end of the kinetic diagram given by Eq. 4a. The required change may be as simple as adding further sequential transitions.

Simulated Gating Current Records

Fig. 3 gives simulated gating current responses of the kinetic model (rate constants as in Fig. 1) in a dynamic steady state at 500 Hz about a series of mean membrane potentials. Because the fit given in Fig. 1 was primarily based on the behavior of the dominant second harmonic of the experimental data, it is not surprising that elements corresponding to the second harmonic are well reproduced in these simulations. The simulations do, however, exhibit features corresponding to a stronger third harmonic than that seen in the data, particularly for mean membrane potentials in the neighborhood of 0 mV. Also, the peak-to-peak amplitude in the simulated gating current decreases somewhat as the mean membrane potential increases (see caption and Discussion). In general, the model tends to hold a relatively constant amplitude throughout the voltage range (see Fig. 2). The experimental data show an almost constant peak-to-peak amplitude as a function of mean membrane potential (see Fohlmeister and Adelman, 1985). In contrast, all of the models presented in the appendix of Fohlmeister and Adelman, 1985 show a very pronounced peak in this amplitude near -35 mV.

Fig. 4 gives simulated gating current responses of the kinetic model for a series of voltage steps from a holding potential of -60 mV. Note the negative (inwardly) directed currents for voltage steps to hyperpolarizing potentials. This is primarily due to a sizable population shift from state x_2 to state x_1 (see Discussion). Stepping in the other direction, the current, i_g, also changes sign. As the level of depolarization increases, the peak current increases, and its duration decreases. As the level of depolarization is increased to values well above 0 mV, the model predicts a reversal in the gating current following its initial large, outwardly directed peak. The reversal is due to the action of the secondary process (see Discussion).

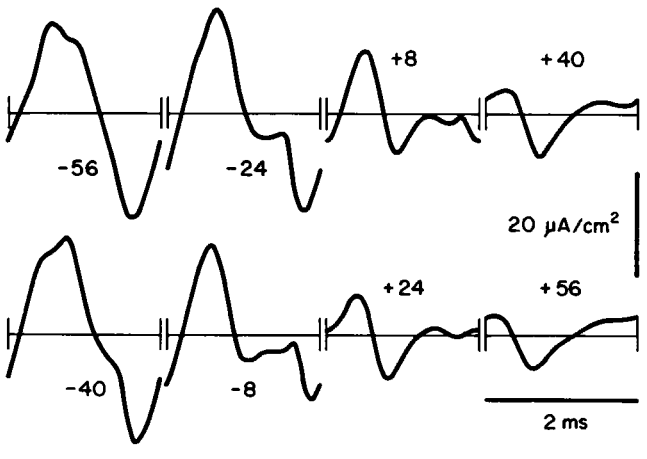

FIGURE 3 Simulated gating currents generated by the model kinetics with parameters as in Fig. 1 for one period in dynamic steady state for eight values of E_{mean}.

Threshold Behavior and Action Potential

To incorporate the kinetic model into a membrane model capable of generating action potentials, at least one of the ten model conformations must be assumed to correspond to an open gate. This role is attributed to the state x_0 irrespective of the relative populations of the substates x_1 through x_5 of the primary process (see Discussion). Fig. 5 gives action potential and subthreshold responses for the model with parameter values corresponding to Fig. 1. The model has been supplemented with sodium inactivation and potassium activation given by the Hodgkin-Huxley model for 8°C. The responses given in Fig. 5 are for instantaneous depolarizations from a resting potential of -60 mV.

It is of some interest to compare the behavior of state variables for sodium activation in the Hodgkin-Huxley model with that of the present kinetic model. Table I gives values of m_∞^3 generated by the Hodgkin-Huxley model, and steady state values of both x_0 and x_5 for -60 and 0 mV. Note that whereas in the Hodgkin-Huxley model nearly all activation gates (89%) are open at 0 mV, the present model predicts only ~30% of the activation gates open. Furthermore, this percentage will not increase substantially in going to higher membrane potentials and may in fact slowly decline for very large E. This is due to the voltage dependence of the rate constants k_{06} and k_{60}; note that κ_{60} decreases and κ_{06} increases with increasing E (Eq. 7a and b), and this retards the further population of x_0 despite the continuing increase in the population of state x_5 with increasing E. The same voltage dependence of k_{06} and k_{60} is also responsible for the difference in the steady state populations of states x_0 and x_5 at -60 mV (see Table I). The conductance ratios of the two models between 0 and -60 mV are $m_\infty^3(0)/m_\infty^3(-60) = 6{,}010$ for the Hodgkin-Huxley model and $x_0(0)/x_0(-60) = 7{,}890$ for the present model with parameters as in Fig. 1.

DISCUSSION

The kinetic model presented in this paper is intended as the simplest physically plausible model of sodium activation gating that is consistent with the behavior of gating currents when driven sinusoidally in dynamic steady states. In arriving at the curves of Fig. 1, no attempt was made to achieve an optimum fit to the experimental curves. The

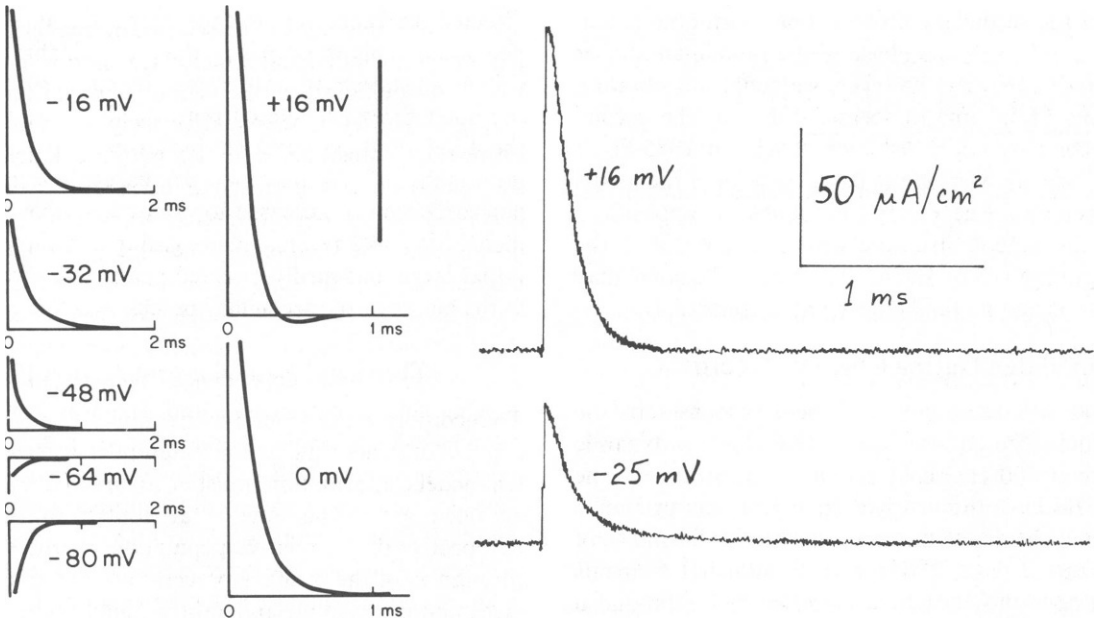

FIGURE 4. *Left:* Model gating currents (parameters as in Fig. 1) generated in response to voltage steps from −60 mV to a series of hyperpolarized and depolarized potentials. Vertical bar is 50 $\mu A/cm^2$. *Right:* Experimental gating current transients in response to depolarizations from a holding potential of −70 mV to +16 and −25 mV. For methods see Fohlmeister and Adelman (1985).

primary reason for this is that the experimental gating currents undoubtedly contain components due to other processes in the membrane (see Fohlmeister and Adelman, 1985). Since these additional processes cannot at this time be compensated for, it is remarkable the degree to which even subtle features of the model simulations agree with the data. These include details in the shapes of the curves of the harmonic data as well as areas of instability. However, we cannot claim that the actual kinetics of gating are necessarily as simple as those presented here. Indeed, it is likely that at least the primary process contains additional conformational substates to account for the discrepancy in the amplitude and phase of the second harmonic at the low end of the experimental range of mean membrane potentials (compare Fig. 7 of Fohlmeister and Adelman, 1985 and Fig. 1 herein).

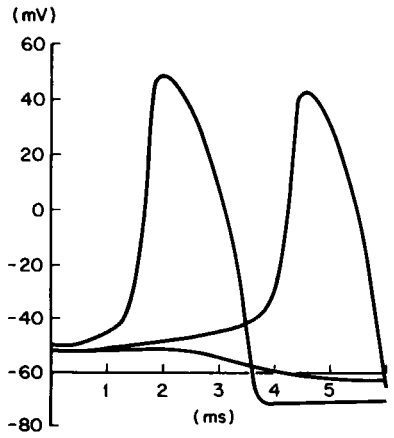

FIGURE 5 Simulated action potentials and a subthreshold response generated by the model with parameters as in Fig. 1 following instantaneous voltage displacements from −60 mV. The model was supplemented with Na inactivation and K activation of the Hodgkin-Huxley model for 8°C. $\bar{g}_{Na}$ = 650 mS/cm². See text for further details.

The two molecular processes involved with activation gating move with independent degrees of freedom. This is expressed mathematically by two independent population constraints (Eqs. 3). Nevertheless, the coupling of the two processes makes the likelihood of a transition between x_0 and x_6 strongly dependent on the state of the primary process that is occupied. Thus, the rate constants of the secondary process include factors of the population probabilities of states of the primary process (Eqs. 2). As a result, the kinetic differential equations are nonlinear (Eqs. 1f, 1g), in contrast to the linear equations of the Hodgkin-Huxley model. Fig. 6 gives the kinetic diagram in terms of the overall molecular conformations where $X_{i,j}$ is the conformation corresponding to molecular substates x_i (i = 1, . . . , 5) of the primary process and x_j (j = 0,6) of the secondary process. Horizontal transitions are strongly voltage dependent. Vertical transition rates are weakly voltage

TABLE I
STEADY STATE VALUES OF STATE VARIABLES FOR SODIUM-ACTIVATION GATING IN THE HODGKIN-HUXLEY MODEL (m_∞^3) AND THE PRESENT MODEL (x_0 and x_5) FOR PARAMETER VALUES CORRESPONDING TO FIG. 1

E[mV]	m_∞^3	x_0	x_5
−60	0.000148	0.000037	0.00000542
0	0.890	0.292	0.292

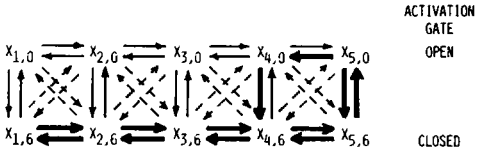

FIGURE 6 Kinetic diagram for model conformational transitions. See text for details.

dependent. Diagonal transitions (dashed arrows) indicate possible coincidental transitions between the primary kinetics (Eq. 4a) and the secondary kinetics (Eq. 4b). Such a coincidence will occur only rarely but cannot be ruled out given the movement of two distinct molecular components with independent degrees of freedom.

One should be cautioned not to confuse gating models that include inactivation gating (see Fig. 5, Stimers, Bezanilla, and Taylor, 1985) with this kinetic diagram, which addresses only the activation gate.

The kinetic diagram satisfies detailed-dynamic-balance in steady state at any fixed voltage. This follows because arrows (rate constants) pointing to the right (or left) in the upper and lower rows of conformations in Fig. 6 are equal pairwise for all voltages. Further, all upwardly (or downwardly) pointing arrows are equal once the substate populations of the primary process have settled into their steady-state values. Thus, net circulation within any kinetic loop is precluded in steady state, thereby avoiding perpetual motion. However, net circulation can occur in dynamic steady state without violation of the second law of thermodynamics because the changing, externally applied field provides the necessary energy source. Indeed, the heavy arrows indicate the most commonly occurring conformational transitions in this model for arbitrary voltage changes in various regions of membrane potential. The locations of these arrows indicate the possibility of net counterclockwise motion around the right-most loop in the diagram; this circulation will occur during sinusoidal oscillation in dynamic steady state for values of E_{mean} for which the periodic gating currents have a bimodal distribution (see Fohlmeister and Adelman, 1985), and is a type of hysteresis effect.

In our attempts to bracket the parameter values with the intent of minimizing the overall differences between model curves and data, we were struck by the tenacity of the model to maintain the basic harmonic features. This is a tribute to the robustness of the model, and gives confidence in the entire approach of harmonic analysis to seek out the general requirements of kinetic structure. Once that structure is determined (or assumed) the harmonic analysis technique is highly sensitive to the values (both relative and absolute) of the rate constants. This is particularly true when areas of harmonic instability exist, such as in the present case. On the other hand, harmonic analysis is apparently quite insensitive to one set of mathematical parameters: The harmonic content in the gating current is a very weak function of the relative mathematical weighting given to individual kinetic transitions provided the weighting remains of the same sign within a kinetic diagram. However, the relative weight assigned to each elementary transition, $x_i \rightleftharpoons x_j$, within a kinetic diagram such as Eq. 4a must correspond to the relative distance that is moved by the charge in that transition. The physical distance moved (component normal to the plane of the membrane) by the charge is in turn reflected in the strength of the voltage dependence of the rate constants for that elementary transition, and harmonic analysis is sensitive to that voltage dependence. This physical argument relating voltage dependence and weighting applies to the movement of a single charge; it does not apply to the movement of a second charge with different magnitude. Thus, the secondary process did require additional weighting (12.0 nano-Coulombs/cm^2). This value was necessary to correctly position the peak in the normalized amplitude of the second harmonic; reducing this weight would shift the peak towards higher values in mean membrane potential, as well as cause some distortion in the curves.

The model presented herein assumes two charged gating particles. To generate the current records of Fohlmeister and Adelman (1985) these particles must have one or the other of the following two properties: (*a*) If the charges are of the same sign, then they must move in opposite directions during either the kinetic transition sequence leading to an open gate following depolarization, or the sequence leading to a closed gate following repolarization. (*b*) If the charges are of the opposite sign, then they must move in the same direction during either of the kinetic transition sequences given in *a* above.

In either case, the sense of the voltage dependencies of the rate constants of the primary process (given by Eqs. 6) and the sense of the voltage dependencies of the rate constants of the secondary process must be opposite, as given by Eqs. 7a and 7b, on purely electrostatic grounds. The model simulations for Fig. 1 satisfy this condition; those for Fig. 2 do not (the simulations of Fig. 2 utilize Eqs. 7c and 7d whose voltage sense is the same as that of the primary process, Eqs. 6). It is remarkable that the physically correct equations lead to harmonic behavior that closely matches the experimental harmonics, whereas the physically incorrect equations do not, despite the fact that the basic harmonic features are generated in both cases. This is additional supporting evidence of the basic correctness of the model kinetic scheme.

The model makes a number of predictions, some of which have been observed in experimental data. One such prediction is that both the magnitude and duration of the gating current at a given depolarized membrane potential will increase if that current is in response to a voltage step from a more hyperpolarized prepotential (see Taylor and Bezanilla, 1983). This is due to the fact that at -60 mV, the state x_2 is considerably more heavily populated than the state x_1; the steady state populations of the primary

kinetic process at −60 mV for parameters as in Fig. 1 are $x_1 = 0.228$, $x_2 = 0.681$, $x_3 = 0.0892$, $x_4 = 0.00193$, and $x_5 = 0.00000542$. Prehyperpolarization will therefore cause a substantial population shift from x_2 to x_1. Subsequent depolarization to the given test potential will then result in a substantial increase in the number of transitions from left to right in Eq. 4a with an attendant increase in the gating current (Eq. 8).

That a state (in this case x_2) other than the left end state of the primary kinetics must be dominantly populated at −60 mV follows directly from the harmonic data. Otherwise, the kinetic system would not allow any substantial transitions to the left (in Eq. 4a) during the bottom half of the sinusoidal voltage swing in dynamic steady state about −60 mV. It is precisely this effect that gives the large second harmonic component at low mean membrane potentials for all of the models in Fohlmeister and Adelman 1985, Appendix. Such behavior is contrary to the data.

Returning now to the model prediction, the increased gating current resulting from hyperpolarized prepotentials will be manifest in a substantial increase in the peak current, but only a slight increase in its duration. The reason lies in the large value of the rate constant k_{12} (= 97.6 ms^{-1} at 0 mV) that is required (in conjunction with a small k_{21}) to prevent the end-state saturation discussed above. Thus, the bulk of the additional gating current will occur early, and the duration of the gating current will be increased by only about 10 μs. Nevertheless, this increased duration is accompanied by a delay in the onset of the open state. Thus, the sodium current will be (sightly) delayed if the test potential is commanded from a prehyperpolarized level. This effect is analogous to (but much smaller than) the Cole-Moore (1960) shift for the potassium channel.

A second prediction is that gating currents in response to voltage steps from rest to well above 0 mV may reverse their direction (sign) following an initial large outwardly directed current as shown in Fig. 4. The initial outwardly directed current is due to charge movement associated with the primary kinetic process, $x_1 \rightarrow x_5$, and the sign reversal is mainly due to the charge movement associated with the transition $x_6 \rightarrow x_0$. Such a reversal is not predicted for depolarizations to $E < +10$ mV (Fig. 4) primarily because the transition $x_6 \rightarrow x_0$ does not contribute a sufficient current component to overcome the continuing outwardly directed current associated with the primary kinetic process.

This prediction must be approached somewhat cautiously. The reason is that a step change in voltage (or in any variable) corresponds to an infinite number of frequency components (the Fourier components of the step). However, the model was constructed on the basis of data obtained for a narrow range of frequencies (0.5 to 3 kHz) in dynamic steady state. As indicated in the Results, the voltage dependence of the rate constants of the secondary process appears to be somewhat frequency dependent. That property must be taken into account in evaluating this prediction.

Perhaps, more importantly, the sign reversal may be obscured by the presence of a gating current component due to the K channel. This slower current could be relatively large at precisely the time during the transient at which the sign reversal is predicted (see Fig. 4). Although the irreversible loss of K conductance in K-free solutions has been reported (Chandler and Meves, 1970), this may be due to the collapse of the K-channel pathway in the absence of conducting ions, with the K-channel gating machinery remaining functional and continuing to generate gating current. If this is the case then dynamic analysis may be useful in separating the gating-current components of the two channels.

A final property of the model relates to single channel data; when a model single channel with the kinetics of Eqs. 1 is gated open in response to a depolarization, the channel may or may not flicker between open and closed (conducting and nonconducting). If it does flicker the lifetime of either state is of the order of 10 μs for parameters as in Fig. 1. The uncertainty of this property lies in the mathematical structure of the rate constants of the secondary kinetic process, $x_6 \rightleftharpoons x_0$, which can be interpreted in one of two ways. This uncertainty reflects the fact that the kinetics describe the probabilistic mass action of many channels acting in concert and contain population probabilities as factors of the rate constants. Predictions of single channel behavior therefore require additional assumptions.

The simplest interpretation of the mass kinetics is that a single channel must be in substate x_5 in order for the transition to the open state, $x_6 \rightarrow x_0$, to occur. Upon entering substate x_5 the transition $x_6 \rightarrow x_0$ will occur on the timescale given by $1/k_{60}$, which is of the order of 5 μs. Because the single channel is now definitely in substate x_5, there is zero probability of the population of substates x_1, x_2, x_3, or x_4, and the inverse transition cannot occur until the channel exits substate x_5. In this interpretation the mean lifetime of the open state is $1/k_{54}$, which equals 0.164 ms at 0 mV, and the conducting state of the channel will not flicker.

However, perhaps a more reasonable physical picture of protein dynamics might favor a more probabilistic interpretation. In that picture, molecular subunits undergo excursions of one or more Ångstroms as a result of thermal vibration within a given conformation (Karplus and McCammon, 1981; Somogyi, Welch, and Damjanovich, 1984). The word conformation is used here as a mean structural arrangement with a lifetime that is long in comparison with the inverse frequency of vibration. In this way the position of the charges associated with the primary kinetics, in particular, will appear diffuse with the possibility of some spatial overlap between conformational substates x_4 and x_5. As a result the rate constants k_{60} and k_{06} retain a probabilistic form such as given by Eqs. 2 even when applied to single channels. In that case the channel

will show brief openings when in substate x_4 and brief interruptions, or bursting, when in substate x_5. The mean lifetime of the interruptions is of the order of 10 μs, based on the magnitude of the rate constants k_{06} and k_{60}, whose values are in turn based directly on the harmonic analysis. Thus, although additional assumptions about protein dynamics must be invoked for interpretation, the model is inherently capable of producing flicker or bursting in the conducting state. Furthermore, the closed state will be virtually silent.

The recent paper by Noda et al. (1984) that gives the primary amino acid sequence of the sodium channel in the electric organ of the eel *Electrophorus electricus* provides a basis for a hypothetical channel and gating process to illustrate a possible mechanism for the above kinetics. Fig. 6 *B* of Noda et al. (1984) gives an array of 24 (presumed) α-helix segments, 16 of which are hypothesized to span the nonpolar portion of the membrane. We propose to fold this array so that the membrane-spanning segments are stably arranged to form a channel as viewed face on to the membrane in Fig. 7 *A*. Note that the segments containing only uncharged residues (filled circles) provide ~74% of the protein surface that is exposed to the membrane lipid (Fig. 7 *B*). The channel itself is lined by segments containing both negatively (aspartic and glutamic acid) and positively charged (lysine and arginine) residues, but with a net (negative) charge of −8. This arrangement appears to provide a stable structure in that there is minimal contact between charged and uncharged segments, and the basically negatively charged segments are spaced by segments containing some positive charge.

The hypothetical gating machinery itself consists of the remaining eight α-helical segments (segments S3 and S4 in each of the four repeating subunits within the primary amino acid sequence; see Noda et al., 1984) plus other elements between repeat units II and III, as defined in Noda et al. (1984), which protrude from the channel wall on the cytoplasmic side. The eight helical segments contain a net excess of 17 positively charged residues and may fold inwards from their anchor points on the channel rim to form a teepee structure with its apex on the extended channel axis (Fig. 7 *C*). This configuration gives a closed

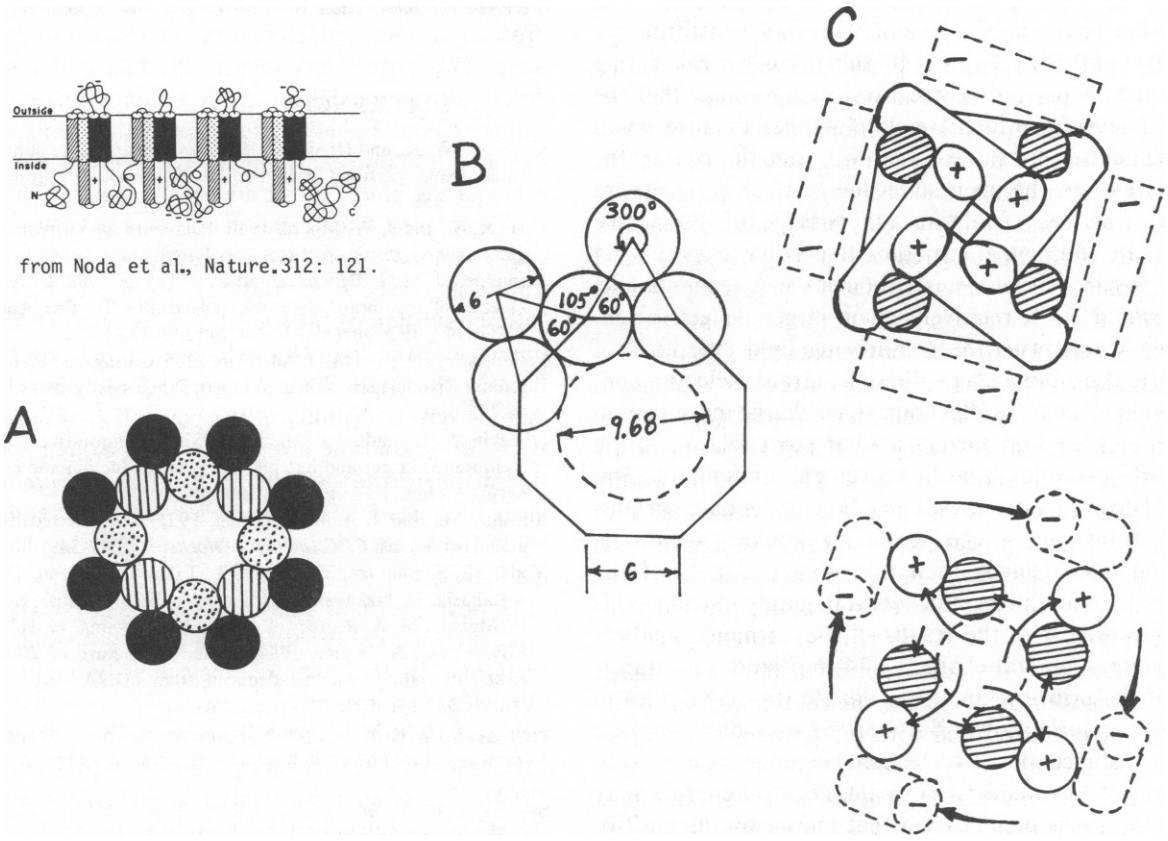

FIGURE 7 (*A*) Hypothetical arrangement of the transmembrane polypeptide segments given in the inset to form a sodium channel as viewed face on to the membrane. Circular elements are coded as in the inset. (*B*) Dimensions of the hypothetical channel assuming α-helical segments whose axes are spaced by 6 Å. (Linear dimensions are in Ångstrom units.) The pore diameter may be reduced to between 5 and 6 Å due to the extension of amino acid residues from the inner layer of segments. (*C*) A hypothetical activation gate extending from the model channel (given in *A*) towards the cytoplasm (out of the page). *Upper* panel = closed gate; *lower* panel = open gate. Uprighting motion of the gate elements is indicated by the arrows in the lower panel. Motion of (−) elements constitutes the primary kinetic process; motion of (+) elements constitutes the secondary kinetic process. *Inset:* Reprinted by permission from *Nature (Lond.)*. 312:121–127. Copyright 1984, Macmillan Journals Limited.

activation gate with positive charge facing the pore opening. The positive residues of segments S4 are so spaced that the charges themselves form a helix of less than one turn around each segment. We postulate that the terminus of this helix at the teepee apex occurs on the external surface, thereby substantially reducing the mutual repulsion among the segments, and simultaneously providing the charge that is attracted by the mechanism of the primary kinetics (see below).

The sequence of residues between repeat units II and III contains four roughly equally spaced subsequences with clustered negative charge. These subsequences are residue numbers 796–806 with 6 negative charges, 847–857 with 6 negative charges, 894–910 with 10 negative charges, and 942–955 with 12 negative charges including an uninterrupted string of nine glutamic acids. These four segments may be spaced around the base of the teepee. In response to a depolarization this large negative charge may move away from the base towards the cytoplasm and constitute the primary process of the gating kinetics. Attracted by this elevated negative charge, the positive segments S4 may pivot outwards on their anchor points, thereby opening the channel by opening the teepee structure at the top. This uprighting rotation of segments S4 may constitute the secondary kinetic process. If this hypothetical gating mechanism is basically correct one might expect that the four segments S3, which are closely linked to corresponding segments S4 at the apex, will remain nearer the channel axis in the open state due to their net negative charge. This will facilitate the passage of permeable cations. In addition, the motion of positive segments S4 occurs, in part, within the extension of the aqueous channel itself, which has a relatively much larger dielectric constant compared with the neighboring lipid (the ratio of dielectric constants being ~40). The larger dielectric constant will enhance the effect of a given charge movement in generating dielectric current at that point relative to the effect of a similar charge movement at some lateral distance from the channel. Thus, this model gate predicts that a transition of the secondary kinetics should be weighted more heavily than that of a transition of the primary kinetics in its contribution to gating current. This correlates well with the results of the harmonic analysis even though the total charge (-34) moved during transitions of the primary kinetics is double (in magnitude) to that moved during a transition of the secondary kinetics, and the distance moved (directional component normal to the plane of the membrane) by the negative charges may be 5 to 10 times greater than that moved by the positive charges as estimated from the voltage dependence of the rate constants.

Inactivation, which has hitherto not been considered, may be due to the movement of protein elements taken from between repeat units I and II, and/or repeat units III and IV. These elements contain a large number of charged residues (32 positive charges and 31 negative charges in total), but as an entity are almost neutral. One can imagine these elements to be situated near the base of the teepee structure for hyperpolarized membrane potential. Following the elevation of the negative charge associated with the primary activation kinetics these inactivation elements may move between the anchor points of segments S3 and S4 towards the channel axis and block the channel opening, thereby inactivating the channel. These inactivation elements would have to be removed from the channel before the negative charge that is associated with the primary activation kinetics could again be seated at the base following repolarization. In this way the two mechanisms of activation and inactivation gating would be coupled, and inactivated channels would generate a reduced gating current due to the steric hindrance experienced by the molecular components associated with the primary activation kinetic process.

Jurgen F. Fohlmeister was supported in part through research grant BNS-8415181 from the National Science Foundation. Computer simulations were supported in part by a grant from the University of Minnesota Computer Center.

Received for publication 18 March 1985 and in final form 23 May 1985.

REFERENCES

Chandler, W. K., and H. Meves. 1970. Sodium and potassium currents in squid axons perfused with fluoride solutions. *J. Physiol. (Lond.).* 211:623–652.

Cole, K. S., and J. W. Moore. 1960. Potassium ion current in the squid giant axon: dynamic characteristic. *Biophys. J.* 1:1–14.

Fernandez, J. M., F. Bezanilla, and R. E. Taylor. 1982. Distribution and kinetics of membrane dielectric polarization II: Frequency domain studies of gating currents. *J. Gen. Physiol.* 79:41–67.

Fohlmeister, J. F., and W. J. Adelman. 1985. Gating current harmonics I. sodium channel activation gating in dynamic steady states. *Biophys. J.* 48:375–390.

Hodgkin, A. L., and A. F. Huxley. 1952. A quantitative description of membrane current and its application to conduction and excitation in nerve. *J. Physiol. (Lond.).* 117:500–544.

Karplus, M., and J. A. McCammon. 1981. The internal dynamics of globular proteins. *CRC Crit. Rev. Biochem.* 9:293–349.

Noda, M., S. Shimizu, T. Tanabe, T. Takai, T. Kayano, T. Ikeda, H. Takahashi, H. Nakayama, Y. Kanaoka, N. Minamino, K. Kangawa, H. Matsuo, M. A. Raftery, T. Hirose, S. Inayama, H. Hayashida, T. Miyata, and S. Numa. 1984. Primary structure of *Electrophorus electricus* sodium channel deduced from cDNA sequence. *Nature (Lond.).*312:121–127.

Somogyi, B., G. R. Welch, and S. Damjanovich, 1984. The dynamic basis of energy-transduction in enzymes. *Biochem. Biophys. Acta.* 768:81–112.

Stimers, J. R., F. Bezanilla, and R. E. Taylor. 1985. Sodium channel activation in the squid giant axon. Steady state properties. *J. Gen. Physiol.* 85:65–82.

Takashima, S. 1978. Frequency domain analysis of asymmetry current in squid axon membrane. *Biophys. J.* 22:115–119.

Taylor, R. E., and F. Bezanilla. 1979. Comments on the measurement of gating currents in the frequency domain. *Biophys. J.* 26:338–340.

Taylor, R. E. and F. Bezanilla. 1983. Sodium and gating current time shifts resulting from changes in initial conditions. *J. Gen. Physiol.* 81:773–784.